Hyperfine Interact
DOI 10.1007/s10751-013-0834-5

Mössbauer and X-ray study of the $Fe_{65}Ni_{35}$ invar alloy obtained by mechanical alloying

R. R. Rodriguez · J. L. Valenzuela · J. A. Tabares · G. A. Pérez Alcázar

Abstract $Fe_{65}Ni_{35}$ samples were prepared by mechanical alloying (MA) with milling times of 5, 6, 7, 10 and 11 h, using a ball mass to powder mass ratio of 20:1 and at 280 rpm. The samples were characterized by X-ray diffraction (XRD) and transmission ^{57}Fe Mössbauer spectrometry. The X-ray diffraction pattern showed the coexistence of one body centered cubic (BCC) and two face centered cubic (FCC1 and FCC2) structural phases. The lattice parameters of these phases did not change significantly with the milling time (2.866 Å, 3.597 Å and 3.538 Å, respectively). After 10 h of milling, the X-ray diffraction pattern showed clearly the coexistence of these three phases. Hence, Mössbauer spectrometry measurements at low temperatures from 20 to 300 K of this sample were also carried out. The Mössbauer spectra were fitted using a model with three components: the first one is a hyperfine magnetic field distributions at high fields, related to the BCC phase; the second one is a hyperfine magnetic field distribution involving low hyperfine fields related to a FCC phase rich in Ni, and the third one is a singlet related to a FCC phase rich in Fe, with paramagnetic behavior. As proposed by some authors, the last phase is related with the antitaenite phase.

Keywords FeNi · Mechanical alloying · Mössbauer spectrometry · Invar composition

Proceedings of the Thirteenth Latin American Conference on the Applications of the Mössbauer Effect, (LACAME 2012), Medellín, Colombia, 11–16 November 2012.

R. R. Rodriguez (✉)
Universidad Autónoma de Occidente, A.A. 2790, Cali, Colombia
e-mail: rubyrocio@gmail.com

J. L. Valenzuela · J. A. Tabares · G. A. Pérez Alcázar
Departamento de Física, Universidad del Valle, A.A. 25360, Cali, Colombia

Published online: 13 March 2013

1 Introduction

The investigation of the magnetic properties of Fe-Ni alloys has a long lasting tradition. New technological methods of preparation and treatment open possibilities to prepare materials with different structures and novel physical properties. This is also the case for the mechanical alloying process, which allows the preparation of nanocrystalline Fe-Ni alloys characterized by a grain size of a few nanometers [1, 2] with a high structural disorder [3–5]. The reduction of the grain size increases the saturation magnetization and decreases the coercivity. In this sense, nanocrystalline Fe-10 and Fe-20 wt.% Ni alloys exhibit a soft magnetic behavior [2].

The as-milled samples, near the invar composition, were characterized by Mössbauer spectrometry (MS) and showed to contain a mixture of α (bcc) and γ (fcc) phases after 48 h of milling [6, 7]. Scorzelli [8] and Valderruten et al. [9] observed a non-magnetic phase usually referred to as "paramagnetic phase". This phase was recently reported by Rancourt and Scorzelli [10] as a possible equilibrium phase in the Fe–Ni system and they propose that this is a low spin γ-Fe–Ni phase (γ_{LS}), with an estimated composition of 25–30 % Ni. Besides, it occurs in close microstructural association with tetrataenite. This phase is only observed by Mössbauer spectrometry because tetrataenite (ordered FeNi) and γ_{LS} (proposed to be called antitaenite) have practically indistinguishable lattice parameters. Therefore, the γ_{LS} phase is not readily observable as a distinct phase by TEM or X-ray diffraction. Additionally Valderruten et al. [9] proposed for this type of Fe-Ni samples a new fitting model, which includes two hyperfine magnetic field distributions (HMFD) corresponding to the two ferromagnetic phases, and a paramagnetic site ascribed to the antitaenite phase.

The aim of the present work is to produce the $Fe_{65}Ni_{35}$ alloy (invar melted composition) by the high-energy ball milling technique. Several alloying times ranging from 5 and 11 h were considered. The powders were investigated by means of X-ray diffraction and ^{57}Fe Mössbauer spectrometry at different temperatures from 20 K up to 300 K.

2 Experimental method

Samples were milled from pure elemental powders (Fe 99.9 % and Nickel 99 %) in a planetary high energy ball mill. The speed used was 280 rpm, and the milling was carried out using a sequence of 60 min milling and 30 min resting. The elemental powders were weighed in stoichiometric proportions, mixed in a small flask and then transferred into the vials under argon atmosphere. We used a 10:1 ball mass to powder mass ratio and the milling times were: 5, 6, 7, 10 and 11 h. XRD measurements were performed using $Cu_{K\alpha}$ radiation and the patterns were fitted using the GSAS software [11] which is based on the Rietveld method combined with Fourier analysis, well adapted for broadened diffraction peaks, and taking also into account instrumental parameters. The refinement of the patterns allows obtaining the lattice parameters, the average grain size and the relative fraction of the different phases. ^{57}Fe Mössbauer experiments were performed on the sample milled during 10 h at 20, 30, 60, 70, 80, 90, 150 and 300 K in transmission geometry using a ^{57}Co/Rh source. The analysis of the Mössbauer spectra was done by using the MOSFIT

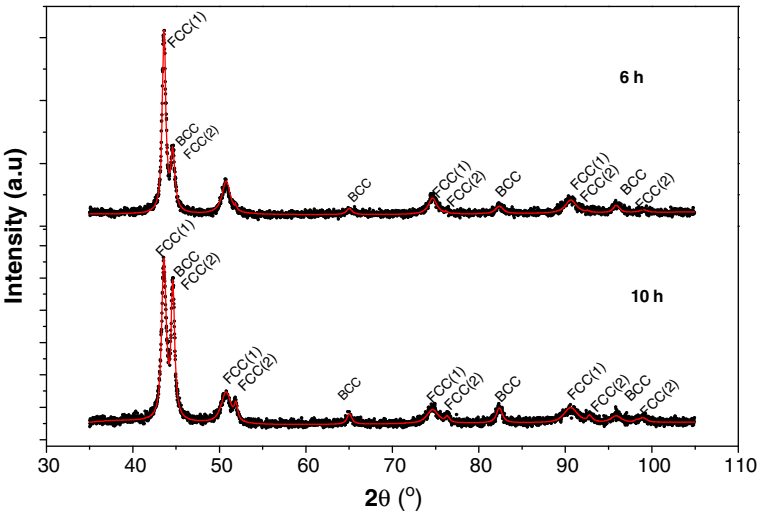

Fig. 1 XRD- patterns for $Fe_{65}Ni_{35}$ milled during 6 and 10 h

program [12] and the values of isomer shift are quoted relative to that of α-Fe at 300 K.

3 Results and discussion

3.1 X-ray diffraction

Figure 1 shows the $Fe_{65}Ni_{35}$ XRD patterns for 6 and 10 h; those corresponding to 5, 7 and 11 h are similar. The XRD patterns exhibit a coexistence of one Body Centered Cubic (BCC) and two Face Centered Cubic (FCC1 and FCC2) structural phases.

The estimation of the lattice parameter and the grain size was obtained from refinement of X-ray patterns using the GSAS procedure. Table 1 shows the observed phases and their respective proportions, and lattice parameters for the different milling times. The lattice parameter of the three phases are approximately constant for the different milling times, the average lattice parameter is 2.866 Å for BCC structure, 3.597 Å for FCC1 (the value reported for the bulk Fe-Ni is 3,5975 Å) and 3.538 Å for FCC2. The lattice parameter of BCC and FCC1 are well in accordance with those reported in Refs. [7, 13]. These two phases are well known in the literature as kamasite and taenite, respectively [1, 14]

Figure 2 shows the variation of Fe-Ni crystallite average size versus time. As can be seen in Fig. 2, during the earlier stages of milling, from 5 h to 7 h, the crystallite size increases, showing that the cold welding predominates over fracture. Afterwards fracture dominates, and the crystallites become smaller. After 11 h the crystallite size was about 15 nm for the three structural phases, according to Scorzelli results [8].

To the best of our knowledge, the FCC2 phase has not been observed by X-ray diffraction by other authors. However, Scorzelli [8], Rancourt and Scorzelli [10] and Valderruten et al. [9] have observed a non-magnetic phase usually referred to

Table 1 Phases, proportions and lattice parameters obtained for the $Fe_{65}Ni_{35}$ alloys milled for different times

Milling time (h)	Phase	Phase (%)	Lattice parameter (Å)
5	BCC	25	2,866
	FCC1	70	3,595
	FCC2	5	3,531
6	BCC	21	2,865
	FCC1	77	3,597
	FCC2	2	3,543
7	BCC	26	2,867
	FCC1	73	3,596
	FCC2	7	3,558
10	BCC	22	2,867
	FCC1	66	3,598
	FCC2	12	3,534
11	BCC	41	2,867
	FCC1	79	3,598
	FCC2	4	3,523

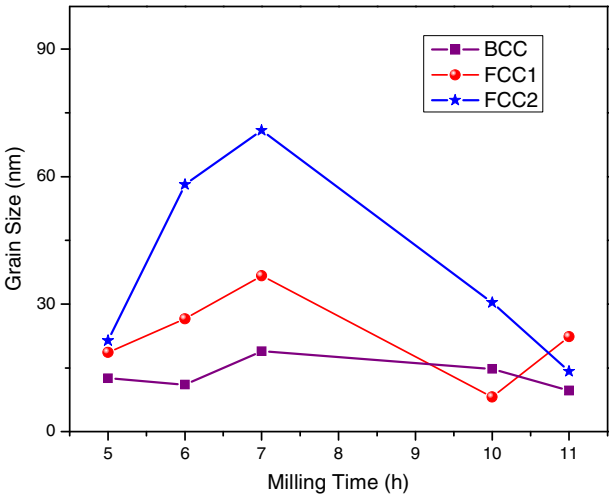

Fig. 2 Grain size of BCC, FCC1 and FCC2 structural phases vs. milling time

as a "paramagnetic phase", which was only observed by Mössbauer spectrometry because tetrataenite (ordered FeNi) and γ_{LS} (proposed to be called antitaenite) have practically indistinguishable lattice parameters.

By X ray-diffraction it was possible to observe that the highest weight percentage of the FCC2 phase was obtained for the sample milled during 10 h. For this reason we decided to study this sample by Mössbauer spectrometry at temperatures in the range from 20 to 300 K.

3.2 Mössbauer spectrometry

The Mössbauer spectra recorded at different temperatures, from 20 to 300 K, and their corresponding hyperfine magnetic field distributions (HMFD's) for the

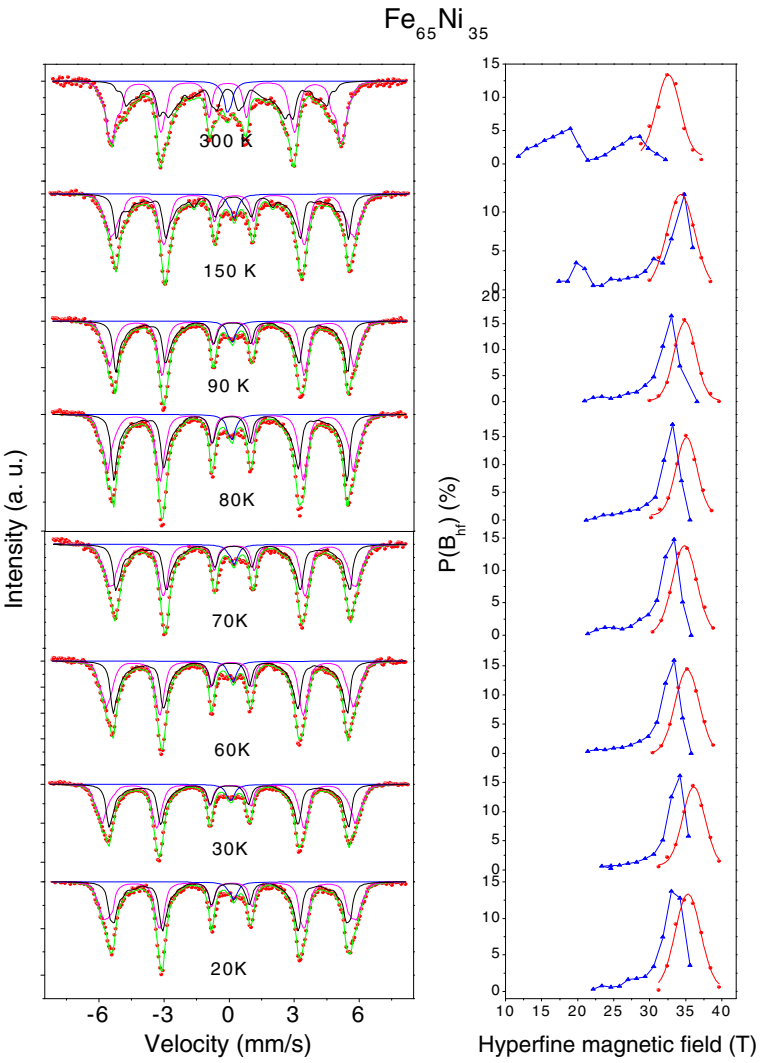

Fig. 3 Mössbauer spectra at different temperatures and their corresponding hyperfine magnetic field distributions, for $Fe_{65}Ni_{35}$ sample milled during 10 h

$Fe_{65}Ni_{35}$ alloys are presented in Fig. 3. Mössbauer spectra were fitted using a model with two hyperfine magnetic field distributions (HMFDs) and one singlet.

In Table 2 are shown the hyperfine parameters obtained from the fitting. The first HMFD, with higher fields, is related to the disordered BCC Fe-Ni phase rich in Fe, and its spectral area at room temperature (46 %) was maintained fixed for all temperatures. The second HMFD, with lower hyperfine fields, is related to the disordered FCC1 phase rich in Ni and the third one, the singlet, was related to the disordered FCC2 phase rich in Fe, with paramagnetic behavior.

Table 2 Hyperfine parameters obtained from the fitting of the Mössbauer spectra: isomer shift (IS), quadrupole splitting (QS), mean hyperfine field (MHF) and area percentage for $Fe_{65}Ni_{35}$ alloy at different temperatures

Temperature (K)	Component	IS (mm/s)	QS (mm/s)	MFH (T)	Area (%)
20	BCC1	0,14	−0,08	35,4	49,0
	FCC1	0,12	0,00	32,2	47,7
	FCC2	0,21			3,3
30	BCC1	0,14	−0,08	36,0	49,0
	FCC1	0,12	−0,02	32,6	47,6
	FCC2	0,19			3,4
60	BCC1	0,13	−0,07	35,2	49,0
	FCC1	0,11	−0,02	31,2	47,3
	FCC2	0,19			3,7
70	BCC1	0,12	−0,07	34,9	49,0
	FCC1	0,10	−0,03	31,5	47,4
	FCC2	0,17			3,6
80	BCC1	0,10	−0,07	35,0	49,0
	FCC1	0,10	−0,02	31,7	47,2
	FCC2	0,16			3,8
90	BCC1	0,09	−0,07	34,9	49,1
	FCC1	0,07	−0,02	31,4	46,9
	FCC2	0,15			4,0
150	BCC1	0,05	−0,07	34,2	49,0
	FCC1	0,05	−0,03	28,9	46,9
	FCC2	0,12			4,1
300	BCC1	−0,06	−0,07	33,3	49,0
	FCC1	−0,06	−0,06	21,4	46,5
	FCC2	−0,01			4,5

We note that the intensity of the singlet decreases with the decrease of temperature. Some Fe sites in the FCC2 phases, with paramagnetic behavior, become ferromagnetic when the temperature decreases.

The two hyperfine magnetic fields distributions, $P(B_{hf})$, obtained from the fitting of the spectra, are shown in Fig. 3. The HMFD with higher fields is related to the BCC structure, rich in Fe. When it was fitted with a Gaussian curve, its central value field was 32.6 T at room temperature, close to that of α-Fe. However, the HMFD contains fields larger than 32.6 T with appreciable probability, showing that the Ni-atoms in the BCC structure increase the ferromagnetic behavior of the Fe-atoms in this phase. This is consistent with what was reported for Fe-Ni disordered alloys [15]. The HMFD with lowers fields, related to the FCC1 ferromagnetic phase, shows two peaks with smaller probabilities than those of the BCC phase. When the temperature decreases the peak with the highest fields slightly shifts to higher fields increasing its probability whereas the one with smaller fields disappears. When the temperature decreases the paramagnetic Fe-atoms in the FCC1 phase, surrounded by Ni-atoms, tend to align with the magnetic field of the ferromagnetic matrix of their neighborhood. This makes those Fe-atoms become ferromagnetic. This tendency increases with decreasing temperature.

The mean hyperfine fields (MHF) of the BCC and FCC1 phases are represented in Fig. 4. The BCC mean hyperfine field at room temperature is higher than that of pure Fe, showing that Ni atoms increase the ferromagnetic behavior of the Fe-

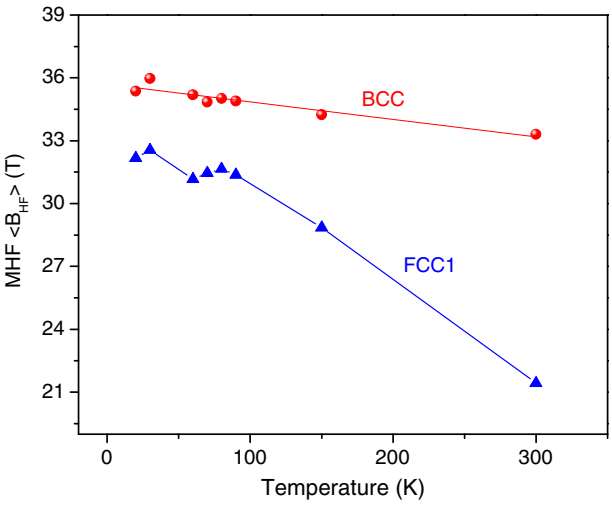

Fig. 4 Mean hyperfine fields of BCC phase and FCC1 phase vs temperature. Line is a guide for the eyes

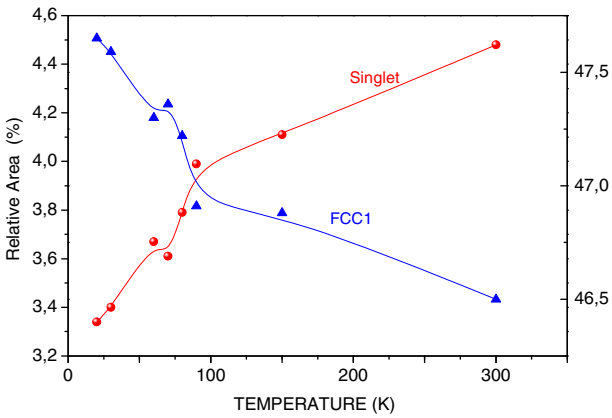

Fig. 5 Relative areas of the singlet and of the HMFD of FCC1 phase vs. temperature. Lines are guides for the eyes

atoms. Also its MHF increases as temperature decreases. The MHF vs. T curve for the FCC1 phase (Fig. 4) is not smooth and shows a clear kink near 60 K (T_k) and a change in slope at about 90 K. When the temperature decreases some spins begin to align due the existence of ferromagnetic exchange interactions. Their number increases as temperature decreases. Due the existence of disorder and competitive interactions which arise from the ferromagnetic exchange between Fe and Ni atoms and the paramagnetic character of Fe-atoms in the FCC structure, some spins tend to remain in the paramagnetic state. For $T > T_k$, these spins are frustrated and show a paramagnetic behavior. Below T_k, these spins are frozen but tend to align with the magnetic field of the ferromagnetic matrix, thereby contributing to the observed average field. Hence, at a given temperature between T_k and 0 K (the re-entrant spin glass region), the average field would be higher than that expected if only ferromagnetic spins were present.

Finally Fig. 5 represents the spectral areas of the paramagnetic site (FCC2) and of the ferromagnetic area of the FCC1 phase, as a function of T. It can be observed

that the paramagnetic area decreases with T, and for T = 60 K a kink appears. The FCC2 spectral area exhibits the opposite behavior, showing that the increase of this spectral area is not only due to the normal increase due to the decrease of T, but also to those paramagnetic sites of the FCC2 phase which become ferromagnetic.

4 Conclusions

$Fe_{65}Ni_{35}$ alloys were prepared by the mechanical alloying technique in a high-energy planetary ball mill. The as-milled samples, characterized by X-ray diffraction, show the coexistence of three phases BCC, FCC1 and FCC2. The last phase is related to the paramagnetic phase obtained by Mössbauer spectrometry. The FCC2 phase is related to the antitaenite phase proposed by Scorzelli. As temperature decreases, the MHF of FCC1 phase increases, and shows a kink near 60 K, which can be attributed to a re-entrant spin-glass phase.

Acknowledgement The authors would like to thank Colciencias, Universidad Autónoma de Occidente and Universidad del Valle for their support.

References

1. Tcherdyntsev, V.V., Kaloshkin, S.D., Tomilin, I.A., Shelekhov, E.V., Baldokhin, Yu.V.: Nanostruct. Mater. **12**, 139–142 (1999)
2. Hamzaoui, R., Elkedim, O., Fenineche, N., Gaffet, E., Craven, J.: Mater. Sci. Eng. **A360**, 299–305 (2003)
3. Hellstern, E., Schultz, L.: J. Appl. Phys. **63**, 1408 (1988)
4. Suryanarayana, C.: Prog. Mater. Sci. **46**, 1–184 (2001)
5. Hellstern, E., Fecht, H.J., Fu, Z., Johnson, W.L.: J. Appl. Phys. **65**, 305 (1989)
6. Djekoun, A., Otmani, A., Bouzabata, B., Bechiri, L., Randrianantoandro, N., Greneche, J.M.: Catal. Today **113**, 235–239 (2006)
7. Valderruten, J.F., Pérez Alcázar, G.A., Greneche, J.M.: J. Phys. Condens. Matter **20**, 485204 (2008)
8. Scorzelli, R.B.: Hyperfine Interact. **110**, 143–150 (1997)
9. Valderruten, J.F., Pérez Alcázar, G.A., Greneche, J.M.: Hyperfine Interact. **195**, 219–226 (2010)
10. Rancourt, D.G., Scorzelli, R.B.: J. Magn. Magn. Mater. **150**, 30 (1995)
11. Larson, A.C., Von Dreele, R.B.: General structure analysis system (GSAS). Los Alamos Natl. Lab. Rep. No. LAUR 86–748 (2004)
12. Teillet, J., Varret, F.: Mosfit Programm, University du Maine, France (unpublished)
13. Petrov, Yu.I., Shafranovsky, E.A., Baldokhin, Yu.V., Kochetov, G.A.: J. Appl. Phys. **86**(12), 7001 (1999)
14. Rancourt, D.G., Lagarec, K., Densmore, A., Dunlap, R.A., Goldstein, J.I., Reisener, R.J., Scorzelli, R.B.: J. Magn. Magn. Mater. **191**, L255–L260 (1999)
15. Restrepo, J., Pérez Alcázar, G.A., Bohórquez, A.: J. Appl. Phys. **81**(8), 4101 (1997)